Undulation Properties of the Lamellar Phase of a Diblock Copolymer: SAXS Experiments

Petr Štěpánek*

Institute of Macromolecular Chemistry, Academy of Sciences of the Czech Republic, Heyrovský Sq. 2, 162 06 Prague 6, Czech Republic

Frédéric Nallet

Centre de recherche Paul-Pascal, CNRS, avenue du Docteur-Schweitzer, F-33600 Pessac, France

Olivier Diat

DRFMC/SI3M/PCI, CEA-Grenoble, 17 avenue des Martyrs, F-38054 Grenoble Cedex 09, France

Kristoffer Almdal

The Danish Polymer Centre, Department of Solid State Physics, Risø National Laboratory, P.O. Box 49, DK-4000 Roskilde, Denmark

Pierre Panine

Installation européenne de rayonnement synchrotron, ESRF, Boîte postale 220, F-38043 Grenoble Cedex, France

Received November 30, 2001

ABSTRACT: We report on X-ray scattering results on an oriented lamellar single crystal of a diblock copolymer melt of poly(dimethylsiloxane)-*b*-poly(ethylene propylene). From the Bragg peak position, q_0, we calculate the temperature dependence of the lamellar period and show that it is in agreement with the values obtained using literature values of the Flory−Huggins parameter, χ. We observe the predicted diffuse scattering affecting the profile of the Bragg peak, which is related to the layer splay and compressional elasticity. We show that extremely small misalignments of the lamellar planes prevent a quantitative calculation of the layer compressibility modulus, B, and we explain this effect qualitatively using the mosaicity theory.

I. Introduction

When a sample of a diblock copolymer melt is cooled from a high-temperature disordered phase into a low-temperature ordered phase, a polycrystalline material is generally formed, consisting of grains of ordered material that are themselves randomly oriented. Orientation of such a sample is then usually achieved by shearing it under appropriate conditions.[1,2] As reported in a previous article, we have succeeded in preparing a macroscopically oriented single crystal of an ordered lamellar diblock copolymer melt good enough for dynamic light scattering experiments.[3] We have thus been able to measure relaxation times of the scattered light as well as their distributions for different orientations of the optical axis of the single crystal with respect to the scattering vector. We have established experimentally the existence of the undulation mode of the lamellar structure, predicted by theory,[4,5] and measured the temperature dependence of its frequency Γ_u as the ODT transition is approached. The frequency of the undulation mode is given[3,4] in terms of the splay elastic constant of the lamellar structure, K, by

$$\Gamma_u = \frac{K}{\eta} q^2 \tag{1}$$

when the scattering wave vector **q** is parallel to the lamellar layers. The temperature dependence of the splay elastic modulus K has thus been determined using known values[3,6] of the viscosity η.

The same oriented block copolymer samples can be used in SAXS experiments. If the X-ray beam is sent parallel to the lamellar layers, a classical 1D Bragg diffraction pattern will appear along the stacking direction. The position q_0 of the first-order maximum is given by

$$q_0 = \frac{2\pi}{d} \tag{2}$$

with d the spacing of the lamellar structure.

In the purely geometric description of the structure as an ideal 1D periodic stack of identical layers, the profile of the Bragg peak is a δ-function smeared by the instrumental resolution. The validity of the geometrical description is limited, however, owing to the prevalence of thermally induced fluctuations. In particular, the undulation mode, discussed above in the dynamic light scattering context, corresponds to fluctuations in the shape of the layers with wave vectors parallel to the layers, whereas the second sound—with wave vectors oblique with respect to the layer plane—is associated with fluctuations in the lamellar spacing.[4] A remarkable aspect of these fluctuations is their ability to change not only the heights of the Bragg peaks but also their *profiles*: it has been shown[7,8] indeed that the Bragg peaks are spread, in a way which is related to the splay elastic modulus K, as well as to the layer compressibility $\bar{B}$ of the lamellar structure. It has thus proven possible[9−13] to determine K and $\bar{B}$ from careful measure-

10.1021/ma0120862 CCC: $22.00
Published on Web 08/15/2002

ments of the profile of the Bragg peaks, i.e., from purely *static* experiments.

In this contribution we report on synchrotron X-ray scattering measurements performed on an oriented sample of a diblock copolymer melt. We study the profile of the first-order Bragg diffraction peak, and we discuss the possibilities of extracting $\bar{B}$ from our results.

II. Theory

The background of our analysis refers to the theory of Amundson and Helfand describing[5] the mechanical properties of lamellar block copolymers. The ordering is considered in the weak segregation limit, with the dimensionless order parameter—the local volume fraction of one component minus its spatially averaged value—taken as a simple sinusoid $\psi = 2A\cos(q_0 z)$ of amplitude A and wave vector q_0 for the undistorted state. The order parameter becomes

$$\psi = 2A\cos[q_0(z-u)] \tag{3}$$

in a distorted state characterized by a layer displacement field u in the z direction normal to the layers.[14] The lamellar structure of a diblock copolymer melt is thus described as analogous to the smectic A phase of thermotropic liquid crystals for which the Landau−de Gennes elastic free energy density is[4] in the harmonic regime

$$\frac{F}{V} = \frac{1}{2}\left\{\bar{B}\left[\frac{\partial u}{\partial z}\right]^2 + K\left[\left[\frac{\partial^2 u}{\partial x^2}\right] + \left[\frac{\partial^2 u}{\partial y^2}\right]\right]^2\right\} \tag{4}$$

From an expansion to the first relevant order of the free energy difference between a distorted state and the reference one, expressions are obtained[5] for the two elastic constants $\bar{B}$ (layer compressibility) and K (splay elastic modulus):

$$\bar{B} = 55.151\rho_c kT\mathrm{A}^2 \tag{5}$$

$$K = 3.6426\rho_c kT {R_g}^2 A^2 \tag{6}$$

with ρ_c the number density of the polymer chains and R_g the radius of gyration. T is the absolute temperature and k the Boltzmann constant. Note that using the theoretical relation[5] between the radius of gyration and the characteristic wave vector $R_g \cong 1.946/q_0$, the two above equations actually lead to

$$\bar{B} = 4{q_0}^2 K \tag{7}$$

Since the degree of segregation between the two blocks—as measured by the amplitude A of the order parameter below the ODT—decreases, approximately linearly, with increasing temperature and discontinuously jumps[5] to zero at the metastability limit of the ordered phase, the elastic moduli should also decrease while approaching the ODT. Large, thermally induced distortions of the lamellar stack are therefore to be expected close to the transition. Peierls[15] and Landau[16] were the first to analyze the anomalous fluctuation properties of a 1D harmonic solid in 3D space, and it was recognized by de Gennes[4] that the smectic free energy, eq 4, somewhat analogous to that of the one-dimensional elastic solid, also leads to an anomalous fluctuation spectrum. The structure factor $S(\mathbf{q})$ theoretically expected for an ideal and infinite smectic A system has been first calculated by Caillé.[7] Its asymptotic behavior in directions parallel (z) or perpendicular ($\perp$) to the layer normal is given by simple power laws:

$$S(0,0,q_z) \propto \frac{1}{|q_z - q_m|^{2-\eta_m}} \tag{8}$$

$$S(q_\perp,0,q_m) \equiv S(0,q_\perp,q_m) \propto \frac{1}{{q_\perp}^{4-2\eta_m}} \tag{9}$$

where $q_m \equiv mq_0$ is the position of the mth harmonic of the structure factor, and $\eta_m \equiv m^2\eta$ is a power law exponent related to the elastic constants K and $\bar{B}$:

$$\eta = {q_0}^2 \frac{kT}{8\pi\sqrt{\bar{B}K}} \tag{10}$$

The intensity of X-ray scattered by a smectic A sample is strictly proportional to the Caillé structure factor when the scattering electrons are located within infinitely thin surfaces. This is no longer the case in the weak segregation limit described by eq 3, since only the first-order harmonic $m = 1$ appears in the scattered intensity. Equations 8 and 9, however, still give the correct asymptotic behavior of the scattered intensity near the first-order Bragg peak.[17] With known values of the splay modulus K from dynamic light scattering, it should thus be possible to determine the layer compressibility $\bar{B}$ by measuring the Caillé exponent η and therefore to check the validity of the theoretical prediction[5] $\bar{B} = 4{q_0}^2 K$ (eq 7).

III. Experiment

Sample Preparation. The diblock copolymer used for this work was poly(dimethylsiloxane)-*block*-poly(ethylene-*co*-propylene) (PDMS−PEP), synthesized by anionic polymerization, as described elsewhere.[6] The molar mass of the polymer is $M_n = 6300$ g/mol, and the fraction of PEP monomers is $f_A = 0.48$. This copolymer has an ODT transition[6] at $T_{ODT} = 64$ °C.

The essential condition for experimental studies of lamellar block copolymers along the lines introduced above is the preparation of a sufficiently large "single crystal" of the ordered block copolymer, free of any defects. Normally, when cooling a block copolymer material from its high-temperature disordered phase into the low-temperature ordered lamellar phase, a "polycrystalline" structure is obtained: the copolymer is arranged in individual grains, each having a typical size of 1−3 μm, depending on the rate of cooling.[18] Each grain has an inner lamellar structure; thus, it is a small uniaxial single crystal, but mutual orientation of the grains is random with lots of defects at the boundaries of the grains.

The single crystal needed for the present work was prepared in a flat capillary of cross section 1 mm × 100 μm (VitroCom, New Jersey). Capillary forces were used to introduce the polymer at a temperature well above the ODT, and the capillary was then sealed. The capillary was placed on the heating stage of an optical microscope. Orientation of the copolymer in a single crystal was achieved by repeated heating and cooling cycles with a rate of 0.01 °C/min in a temperature interval of about 1 °C around the ODT, observing the quality of orientation by polarized microscopy. Once the orientation was achieved, the capillary was slowly cooled to room temperature with a rate of 0.1 °C/min. In such a macroscopically oriented state, the layers are parallel to the flat surfaces of the capillary (homeotropic orientation).

Small-Angle X-ray Scattering. A series of small-angle X-ray scattering (SAXS) experiments were performed on the High Brilliance beam line ID2[19] at the ESRF (Grenoble, France). The SAXS setup is based on a pinhole camera with a beam stop placed in front of a two-dimensional detector (image

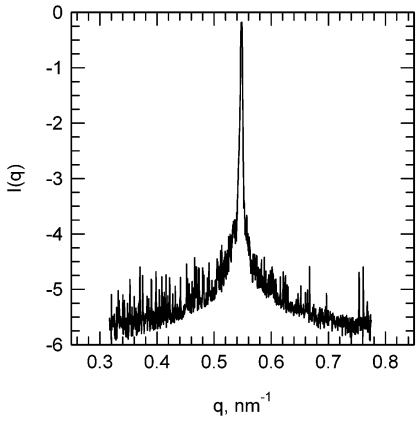

Figure 1. Dependence of the scattered intensity $I(q)$ (in logarithmic scale) on the scattering vector q in the horizontal plane for the PDMS−PEP-6 diblock copolymer at a temperature of 58 °C. The location of the first-order Bragg peak is very precisely defined to be $q_0 = 0.5479 \pm 0.0001$ nm^{-1}.

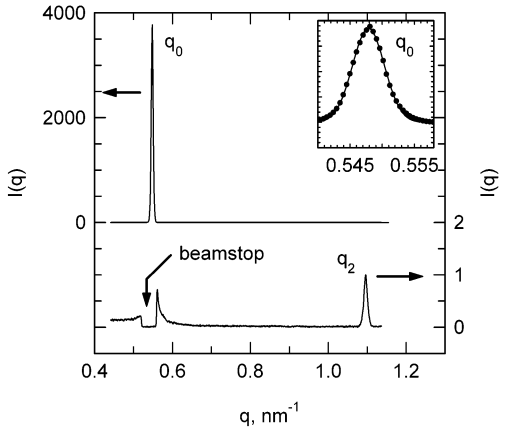

Figure 2. Comparison of first- and second-order peaks of the scattered intensity $I(q)$ for the same conditions as in Figure 1. A Gaussian fit gives $q_1 \equiv q_0 = 0.5479$ nm^{-1} and $q_2 = 1.0961$ nm^{-1}. For obtaining a sufficient dynamic range at the second-order peak, a beamstop was introduced to hide the first-order peak. In this configuration, the direct beam was outside the detector. The inset shows details of the first-order peak; with the high resolution available on the beamline ID2, the position can be determined accurately to the fourth decimal place.

plate or X-ray image intensifier coupled to a CCD camera). The X-ray scattering patterns were recorded on the detector that was most of the time located at 6 m from the sample, using a monochromatic incident X-ray beam (wavelength $\lambda =$ 0.1 nm). The available wave vector range was 0.17−0.91 nm^{-1}. The long axis of the capillary was vertical, and a rotating stage allowed setting the flat surfaces of the capillary either parallel to the incident horizontal beam (planar configuration) or perpendicular to it (homeotropic configuration). The shape of the beam incident on the capillary is fixed by rectangular slits, with slit apertures 200 μm vertically and 15 μm horizontally.

IV. Results and Discussion

In the planar configuration, the scattering patterns obtained at temperatures below ODT show two first-order Bragg peaks located symmetrically at $\pm q_0$ in the horizontal plane and negligible scattering outside this plane. Figure 1 shows a typical dependence of the scattered intensity $I(q)$ on the wave vector q in the neighborhood of q_0 obtained as a cut of the two-dimensional scattering pattern along the horizontal axis. In the same plane, *extremely weak* second-order peaks located at $\pm 2q_0$ can be observed at room temperature, changing specially for that purpose the sample-to-detector distance to 4 m. As the intensity ratio between the second- and first-order peaks is typically 2.5×10^{-4}, a beamstop was introduced to hide the first-order peak and obtain a sufficient dynamic range without saturating the detector; cf. the example displayed in Figure 2. Only background scattering was observed when the sample was rotated in the homeotropic configuration. These features confirm that the block copolymer melt is indeed in a one-dimensionally ordered, lamellar phase. The weakness of the second-order maximum may be taken as an indication that the sinusoidal composition profile of the weak segregation limit theory[20] (WSL) is a good approximation of the structure—harmonic profiles do not yield any higher order reflections—even though a nearly symmetric, square-well electron density profile (appropriate in the case of *strong segregation*) would also lead to a negligible second-order intensity. We do not have data, unfortunately, in the wave vector range where the *third* order peak—if any—should be expected. We nevertheless believe that the WSL is the relevant regime in our system, since on the basis of the χ values estimated below, the present experiments are performed in the range $\chi N = 14-16$.

The temperature dependence of the lamellar spacing, d, derived from the experimentally determined position of the first-order Bragg peak, q_0, is plotted in Figure 3. The lamellar spacing d increases as temperature is decreased deeper below ODT, which is presumably due to increasing incompatibility of the two blocks. In the strong segregation regime, the mean-field theory[21] provides an explicit relation between d and the Flory−Huggins interaction parameter of the blocks, χ:

$$d_{\text{lamellar}} = 1.10 a N^{2/3} \chi^{1/6} \qquad (11)$$

with a segment length a and a number of segments N. In the weak segregation regime, near the ODT, there is also a way of relating the lamellar spacing d to χ. It has been established[22] that the same eq 11 provides a reasonable and internally consistent estimate of χ for the weak and intermediate segregation regimes: Matsen and Bates[20] calculated d using self-consistent mean-field theory without the traditional approximations and have found that the results differ from eq 11 by only about 20% when $\chi N = 10$ and by 5% when $\chi N = 40$. The temperature dependence of χ for this polymer, $\chi = A/T + B$ (with $A = 64$ and $B = -0.03$), was determined[23] by comparing ODT temperatures of copolymers with different molecular weights. Using eq 11, we can then calculate the expected temperature dependence of lamellar spacing d. We obtain $d = 11.66$ nm at 25 °C and $d = 11.43$ nm at 60 °C. These values are in good agreement with the data shown in Figure 3, the difference being less than 3%. For this calculation, we have chosen[23] $N = 106$ and used temperature-dependent values of a. Returning to Figure 3, we observe that there is a small increase or at least leveling of the lamellar period in the immediate vicinity of the ODT. It is associated with a sharp decrease in peak intensity, as shown in the inset of Figure 3. Although this increase is only about 0.2%, it seems to be quite systematic in a narrow temperature region (~1 °C) just below ODT. We have no exhaustive explanation for these features at the present time, but they might be related to a rearrangement of chain conformations just before melting, simi-

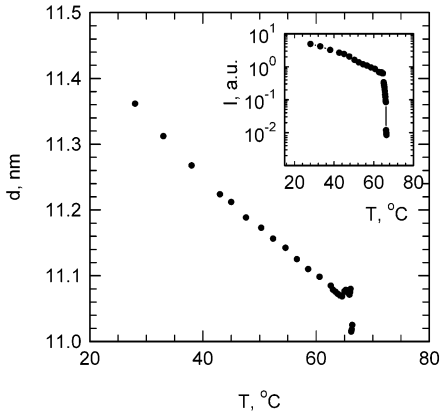

Figure 3. Temperature dependence of the lamellar spacing d—as calculated from eq 2—and of the intensity at the Bragg peak (inset).

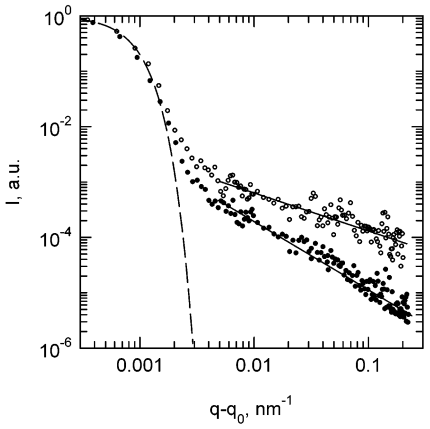

Figure 4. Normalized intensity profile of the Bragg peak, close to $q_z = q_0$ in logarithmic coordinates. The symbol (●) corresponds to a temperature of 30 °C and the symbol (○) to 57 °C. Because of the logarithmic scale, 10 data points have been averaged for $q - q_0 > 0.01$ nm^{-1}. The dashed line is a Gaussian fit to the Bragg peak in the region where the intensity exceeds 1% of its peak value. The full lines are linear fits for $q - q_0 > 0.005$.

larly to what is occasionally observed[24] in the vicinity of the crystallization temperature.

The profile of the first-order Bragg peak in the horizontal plane, for $q > q_0$, is shown in Figure 4 at two different temperatures. The expected diffuse scattering is clearly observed as a marked deviation of the peak profile from the Gaussian form. The intensity of the diffuse scattering is very weak, of the order of 10^{-3} of the peak intensity or less, but its value is significantly above the background level. The diffuse scattering increases relative to the peak intensity as the temperature gets closer to the ODT temperature. There is a substantial scatter in the data at larger values of $q - q_0$; nevertheless, it was possible at all temperatures to fit a straight line (i.e., a power law decay) into the asymptotic parts of the curves. Considering the simple scheme presented in section II, cf. in particular eq 8, the slope of this line defines an exponent written as $2 - E$. The exponent E is plotted as a function of temperature in Figure 5a. Despite some scatter in the data due to the rather small intensity of the diffuse scattering, we observe a clear increase of E with increasing temperature.

Using eq 7 and known values of K, it should be possible to extract $\bar{B}$ from the experimentally determined values for E, with the identification $E \equiv \eta$. This

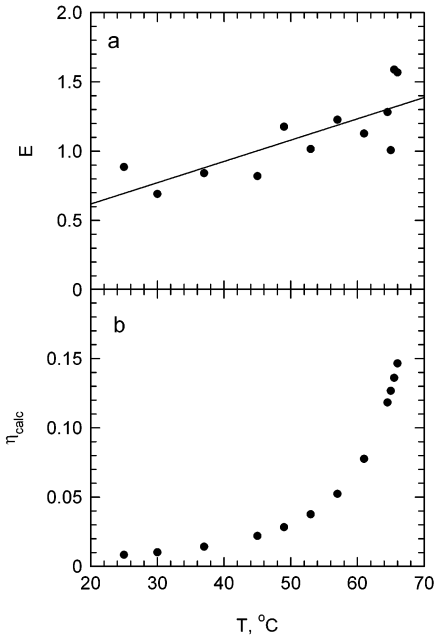

Figure 5. (a) Temperature dependence of the experimentally determined Caillé exponent E. (b) Calculated values of the Caillé exponent η_{calc} using eq 12.

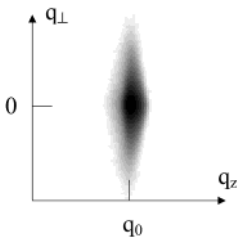

Figure 6. Diffraction spot of the first-order Bragg peak obtained at $T = 30$ °C. The intensity is represented on a logarithmic scale.

procedure, however, leads to "unreasonably" small values of $\bar{B}$. To understand this problem, we calculate the *expected* values of the Caillé exponent η_{calc}, using eq 10 into which we insert values of q_0 obtained from the lamellar distance d (Figure 3) and values of K measured by dynamic light scattering (Figure 5 in ref 3). We also make use of the theoretical relation $\bar{B} = 4q_0^2K$ (cf. eq 7, section II), assuming it to be correct in order to recast eq 10 into the convenient form:

$$\eta_{calc} = \frac{q_0 kT}{16\pi K} \tag{12}$$

In Figure 5b we plot the values of η_{calc} obtained in this way. The experimental values of E shown in Figure 5a are about an order of magnitude *larger* than the values predicted by eq 12. In the following we explain that this discrepancy between E and η_{calc} probably results from small remaining imperfections in the alignment of the single crystal.

The *2-dimensional* image of the first-order Bragg peak in the plane of the detector is displayed in Figure 6 with logarithmic intensity units. The transverse scan of the Bragg spot displayed in Figure 7, rather close to a Lorentzian line shape, indicates that the relatively important extension of the Bragg peak in the $q_\perp$ direction is more likely due to tiny imperfections in the crystal alignment than to the true Caillé diffuse scattering. These imperfections are schematically repre-

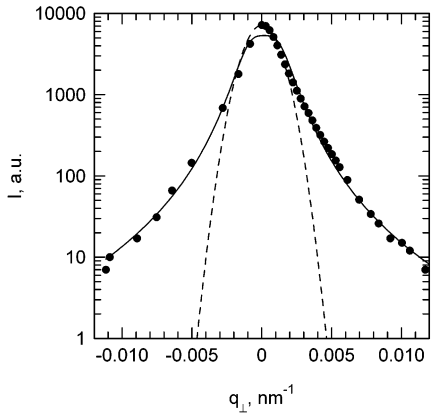

Figure 7. Scan of the Bragg spot in the $q_\perp$ direction. The dashed line corresponds to a Gaussian fit; the line shape is much better described by a Lorentzian law (full line).

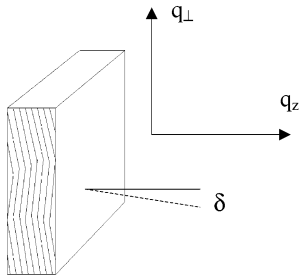

Figure 8. Schematic representation of the postulated misalignment of the lamellar planes.

sented in Figure 8. We define the angle δ as the angle in the vertical plane between the local normal to the layers with the nominal q_z direction. In a polarizing microscopy observation, the texture described in Figure 8, reminiscent of the texture resulting from the well-known *undulation instability* of smectic A liquid crystals,[4] looks probably hardly different from the perfectly aligned state for small distortion angles δ. It cannot be resolved either with our X-ray experiment, except in the special case where the undulation instability is deliberately induced by a thermal shock applied to the sample. In this latter case, transitory lattices of parabolic focal conics (PFC) appear[25] in the sample, leading to a significant splitting of the Bragg peak into two spots slightly above and below the nominal q_z axis. For thermally relaxed samples, the misalignment thus remains very weak. We estimate it from the extent of scattering along the $q_\perp$ direction in Figure 6. Ignoring for this purpose any diffuse scattering, we find that the point where the intensity has decreased to $I = I_{max}/e$ corresponds to $\delta = 1°$, while I decreases to $I_{max}/1000$ for $\delta = 6.2°$. These values do not change when varying the temperature, once the sample is thermally relaxed.

The impact of structural imperfections on diffuse X-ray scattering in smectic liquid crystals has been theoretically studied in ref 26. It is shown that, in the particular case of randomly oriented domains, eqs 8 and 9 are both replaced by a unique equation

$$S_{\text{random}}(q) \propto \frac{1}{|q - q_m|^{1-\eta_m}} \qquad (13)$$

with a much weaker power-law singularity in eq 13 than in its anisotropic counterparts. For an oriented lamellar structure with a small mosaicity described as a Gaussian distribution of orientations, the structure factor along the nominal q_z direction is given by[26]

$$S_{\text{mosaic}}(0,0,q_z) \propto \frac{1}{|q_z - q_m|^{M_m}} \qquad (14)$$

with a well-defined "mosaic" exponent M_m equal to $1 - \eta_m$ for $q_z \ll q_c$ and equal to $2 - \eta_m$ in the opposite limit; the singularity is no longer a power law in the intermediate range. The crossover wave vector q_c varies quadratically with the mosaicity angle. In our experiment, unfortunately, the mosaicity[26] cannot be described as Gaussian (see Figure 7), and we have no definite way to model the shape of the Bragg singularity. On a qualitative basis, the observed apparent exponent M_m will be intermediate between the two extreme values $1 - \eta_m$ and $2 - \eta_m$. This explanation of the discrepancy between E and η_{calc} shows how delicate is the description of order in soft materials. The main finding of this work—the description of the diffuse scattering near the first-order Bragg peak in a lamellar block copolymer—remains however unaffected by the unfortunate difficulty of a quantitative calculation of the Caillé exponent.

V. Conclusions

Small-angle X-ray scattering experiments have been performed on an oriented sample of the lamellar phase of a diblock copolymer as a function of the temperature. Except very close to the ODT, the small but significant variation of the smectic period is in a quantitative agreement with the temperature dependence of the Flory–Huggins interaction parameter χ obtained earlier. We have also been able to observe qualitatively the predicted broadening of the Bragg peak in the form of a Caillé wing, which is related to the layer splay and compressibility moduli of the lamellar structure. As temperature of the system is increased toward the ODT, the amplitude of the Caillé wing increases, indicating a decrease in the elastic moduli. A discrepancy was found between the calculated and observed values of the Caillé exponent that prevented a quantitative calculation of the layer compressibility modulus $\bar{B}$. We have shown that this effect could be explained by small imperfections in the alignment of the smectic planes, the consequences of which have been predicted theoretically and are in reasonable agreement with our findings.

Acknowledgment. The SAXS experiment has been performed at the European Synchrotron Radiation Facility, experiment SC-672. We have received financial support by the Grant Agency of the Czech Republic (Grant 203/99/0573) and by the French CNRS (Award 7907).

References and Notes

(1) Koppi, K. A.; Tirrel, M.; Bates, F. S. *Phys. Rev. Lett.* **1993**, *70*, 1449.
(2) Maring, D.; Wiesner, U. *Macromolecules* **1997**, *30*, 660.
(3) Štěpánek, P.; Nallet, F.; Almdal, K. *Macromolecules* **2001**, *34*, 1090.
(4) de Gennes, P. G. *The Physics of Liquid Crystals*; Clarendon Press: Oxford, 1974.
(5) Amundson, K.; Helfand, E. *Macromolecules* **1993**, *26*, 1324.
(6) Almdal, K.; Mortensen, K.; Ryan, A.; Bates, F. S. *Macromolecules* **1996**, *29*, 5940.
(7) Caillé, A. *C. R. Acad. Sci. Paris* **1972**, *B274*, 891.

(8) Gunther, L.; Imry, Y.; Lajzerowicz, J. *Phys. Rev. B* **1980**, *22*, 1733.
(9) Als-Nielsen, J.; Litster, J. D.; Birgenau, R. J.; Kaplan, M.; Safinya, C. R.; Lindegaard-Andersen, A.; Mathiesen, S. *Phys. Rev. B* **1980**, *22*, 312.
(10) Roux, D.; Safinya, C. R. *J. Phys. (Paris)* **1988**, *49*, 307.
(11) Nallet, F.; Laversanne, R.; Roux, D. *J. Phys. II* **1993**, *3*, 487.
(12) Oda, R.; Litster, J. D. *J. Phys. II* **1997**, *7*, 815.
(13) Bouglet, G.; Ligoure, C. *Eur. Phys. J. E* **1999**, *4*, 137.
(14) Note that this description incorporates via the layer displacement variable *u* the so-called *statistical structure of interfaces*, as considered for example in Semenov, A. N. *Macromolecules* **1994**, *27*, 2732 for the simple case of an interface between two immiscible polymers.
(15) Peierls, R. E. *Helv. Phys. Acta* **1974**, *7* (Suppl. 11), 81.
(16) Landau, L. D. In *Collected Papers*; Ter Haar, D., Ed.; Gordon and Breach: New York, 1965; p 209.
(17) Nallet, F.; Roux, D.; Milner, S. T. *J. Phys. (Paris)* **1990**, *51*, 2333.
(18) Garetz, B. A.; Newstein, M. C.; Dai, H. J.; Jonnalagadda, S. V.; Balsara, N. P. *Macromolecules* **1993**, *26*, 3151.
(19) Bösecke, P.; Diat, O. *J. Appl. Crystallogr.* **1997**, *30*, 867.
(20) Matsen, M. W.; Bates, F. S. *Macromolecules* **1996**, *29*, 1091.
(21) Semenov, A. N. *Sov. Phys. JETP* **1985**, *13*, 602.
(22) Ren, Y.; Lodge, T. P.; Hillmyer, M. A. *Macromolecules* **2000**, *33*, 866.
(23) Vigild, M. Ph.D. Thesis, Risø, Denmark, 1997.
(24) Baldrian, J., private communication.
(25) Rosenblatt, C. S.; Pindak, R.; Clark, N. A.; Meyer, R. B. *J. Phys. (Paris)* **1977**, *38*, 1105.
(26) Kaganer, V. M.; Ostrovskii, B. I.; de Jeu, W. H. *Phys. Rev. A* **1991**, *44*, 8158.

MA0120862